ISSN 0021-3640, JETP Letters, 2022, Vol. 115, No. 4, pp. 186–189. © The Author(s), 2022. This article is an open access publication, corrected publication 2022.
ISSN 0021-3640, JETP Letters, 2022. © Pleiades Publishing, Inc., 2022.
Russian Text © The Author(s), 2022, published in Pis'ma v Zhurnal Eksperimental'noi i Teoreticheskoi Fiziki, 2022, Vol. 115, No. 4, pp. 213–217.

OPTICS
AND LASER PHYSICS

Resonant Hybrid Metal–Dielectric Nanostructures for Local Color Generation

E. I. Ageev[a], *, V. A. Iudin[a], Y. Sun[a], E. A. Petrova[a], P. N. Kustov[a], V. V. Yaroshenko[a], J. V. Mikhailova[a], A. S. Gudovskikh[b], I. S. Mukhin[a, b], and D. A. Zuev[a]

[a] *ITMO University, St. Petersburg, 197101 Russia*
[b] *Alferov University, St. Petersburg, 194021 Russia*
**e-mail: eiageev@itmo.ru*

Received December 3, 2021; revised January 12, 2022; accepted January 12, 2022

Here, we experimentally and theoretically demonstrate a laser-induced change in local color based on the reshaping of gold–silicon asymmetric nanostructures. The evolution of scattering properties enabled by laser reshaping shows the potential of hybrid metal–dielectric nanostructures for color printing applications. The reshaping process can tune the resonance of the nanostructure in the wavelength range between 500 and 800 nm resulting in different colors of illuminated nanostructures. Moreover, the modeling of the scattering diagram of hybrid nanoparticles before and after femtosecond laser reshaping shows that color tuning is simultaneously accompanied by substantial reconfiguration of the distribution pattern for both peaks in the scattering spectrum.

DOI: 10.1134/S0021364022040014

Structural colors are based on the interference between visible light and periodical microstructures on the order of the wavelength, and many examples could be found in nature and daily life. Lately, it also includes colors from light interaction with individual subwavelength resonators like nanoantennas [1]. The origin of colors comes either from localized surface plasmon resonance (LSPR) in the case of interaction between light and metallic nanostructures [2, 3] or can be supported by Mie resonance in all-dielectric structures [4, 5].

In the case of metallic structures supporting LSPR, the resulting color (resonance frequency) is dependent on the particle's geometry, size, and environment [6]. Typical metals used for plasmonic colors (gold, silver, and aluminum [7–9]) inherently suffer from Ohmic losses that have an impact on optical resonances followed by limited color gamut. However, a ≈50% of sRGB color gamut was reported with the use of gap plasmon resonators [9].

A high-index dielectrics/semiconductors supporting Mie resonances and possessing negligible optical losses are alternative to plasmonic structures. Typical materials here are silicon nitride (SiN) [10], silicon (both hydrogenated amorphous (α-Si:H) [11] and crystalline (c-Si) [12]) and titanium oxide (TiO_2) [13], where high-quality-factor resonances can appear.

Metal–dielectric (hybrid) nanostructures accommodate the advantages of both parts and possess some properties (for example, strong nonlinear optical properties [14]), which are essential in the context of practical applications. For such structures, it is possible to overlap plasmon mode with electrical dipole (ED) and magnetic dipole (MD) resonances of the silicon nanocone by gradually changing the shape of the metallic component under the highly precise femtosecond laser melting at the nanoscale. It was demonstrated for single metal–dielectric (Au/Si) nanoparticles [15], dimers [16], and oligomers [17], providing strong manipulation of their optical properties such as scattering and near field distribution.

However, identical nanostructures can be used to local colorate the surface and make it possible to change the color after fabrication. Such tuning can be enhanced by the presence of resonances from both gold and silicon parts. Moreover, color tuning is simultaneously accompanied by alteration in light scattering patterns. In this letter, we both experimentally and theoretically demonstrate a laser-induced change in local color.

The left side of Fig. 1 shows the concept of laser-induced reshaping where the initial gold nanoparticles in the shape of nanodisks are located on truncated silicon cones forming the hybrid asymmetric nanostructure. The method of hybrid nanostructures fabrication was developed in [15] using electron beam lithography to produce the arrays of metal nanodisks consisting of Cr/Au layers and radio-frequency inductively coupled plasma technology to etch the silicon layer through a fabricated metal mask. The typical SEM image of the

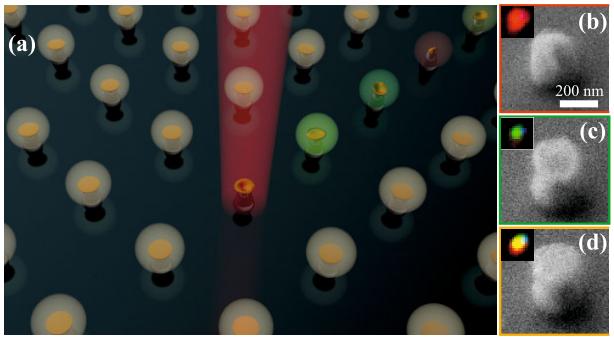

Fig. 1. (Color online) (a) Concept of laser-induced reshaping and characteristic SEM images of hybrid nanostructures (b, c) after and (d) before modification. Insets show a micro image observed in a dark field illumination.

fabricated hybrid structure is presented in Fig. 1d, a yellow frame.

To provide a reshaping of hybrid nanostructures, a commercial femtosecond laser system (femtosecond oscillator TiF-100F, Avesta Project) was used, providing laser pulses at 790 nm central wavelength (FWHM ≈ 11 nm), with maximum pulse energy of 5 nJ, and pulse duration of 100 fs at the repetition rate of 80 MHz. Laser energy was varied and controlled by an acousto-optical modulator (R23080-3-LTD, Gooch and Housego) and a power meter (FielfMax II, Coherent), respectively. Here, a repetitively-pulsed exposure is used based on an acousto-optical modulator. It is open for 2 μs; and the structures are irradiated during the scanning process. After all, the structures in the laser spot area are exposed to $\approx 10^5$ pulses. At the same time, the pulse duration was measured by an autocorrelator (Avesta Project). Laser pulses were focused with Olympus 40x, NA = 0.75 objective. The samples were placed on a three-dimensional air-bearing translating stage driven by brushless servomotors (ABL1000, Aerotech), allowing sample translation with accuracy around 0.1 μm.

Reshaping of gold nanoparticles in hybrid nanostructures using femtosecond laser irradiation is based on the dewetting process. The experiment showed that the irradiation regime could be chosen so that only gold nanoparticles are reshaped from nanodisks to nanocups, while the truncated silicon cone remains unchanged. This is due to the relatively higher melting temperature and enthalpy of silicon fusion (about 1687 K and 50.21 kJ/mol in contrast to 1337 K and 12.55 kJ/mol for gold). Additionally, a very thin 2 nm Cr film prevents the changing of gold nanoparticles' volume. Here, during the reshaping process, the structures were treated with different fluences in the range of 20–100 mJ/cm^2 (Figs. 1b, 1c).

Preliminary optical imaging of the structures was provided immediately during the laser processing by an integrated CCD camera. The high-resolution morphology characterization was carried out through a

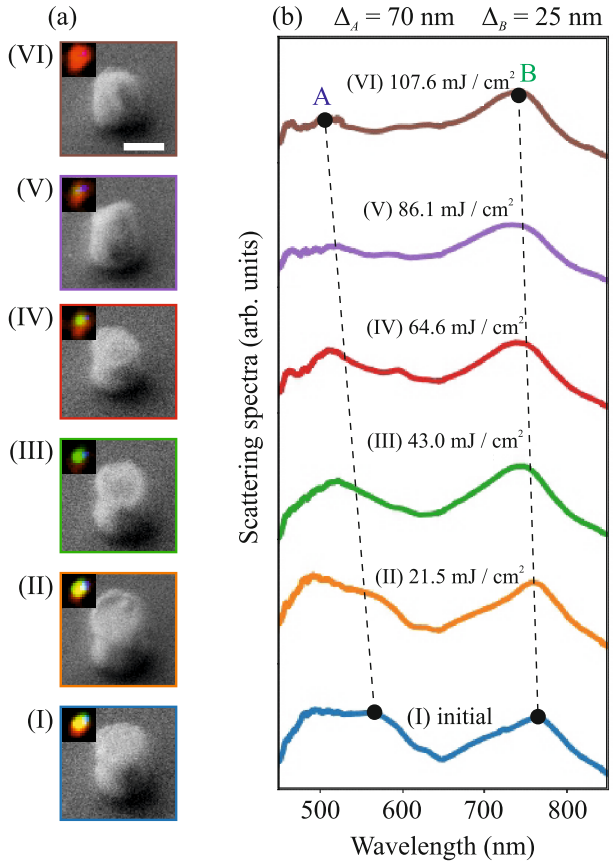

Fig. 2. (Color online) (a) Side view SEM images and (b) measured scattering spectra of a typical hybrid structures before and after processing with various laser fluences: (I) initial, (II) 21.5, (III) 43.0, (IV) 64.6, (V) 86.1, and (VI) 107.6 mJ/cm^2. The white line corresponds to 200 nm.

scanning electron microscope (SEM, Carl Zeiss, Neon 40). Scattering spectra measurements were carried out in a dark-field scheme. The arrays irradiation was performed by non-polarized light from a halogen lamp (Avantes AvaLight-HAL-S-Mini) at an incidence angle of 70° with surface normal focused with Mitutoyo Plan Apo NIR, 10x, NA = 0.26 objective. The scattered signal collection was performed utilizing objective Mitutoyo Plan Apo NIR HR, 100x, NA = 0.7, which directed light to a commercial spectrometer (Horiba LabRam HR) with 150-g/mm and 600-g/mm diffraction gratings, equipped with a CCD camera (Andor DU 420A-OE 325). A confocal optical scheme was optimized for signal collection from individual nanostructures.

Figure 2a shows side-view SEM images of typical structures after processing with various laser fluences presented in the caption. As can be seen from the figure, the hybrid structures are just slightly modified within 20 mJ/cm^2 exposure. However, when the nanostructures are illuminated with a femtosecond laser beyond 40 mJ/cm^2, it starts melting and reshapes as nanocups. Moreover, with further increase in the flu-

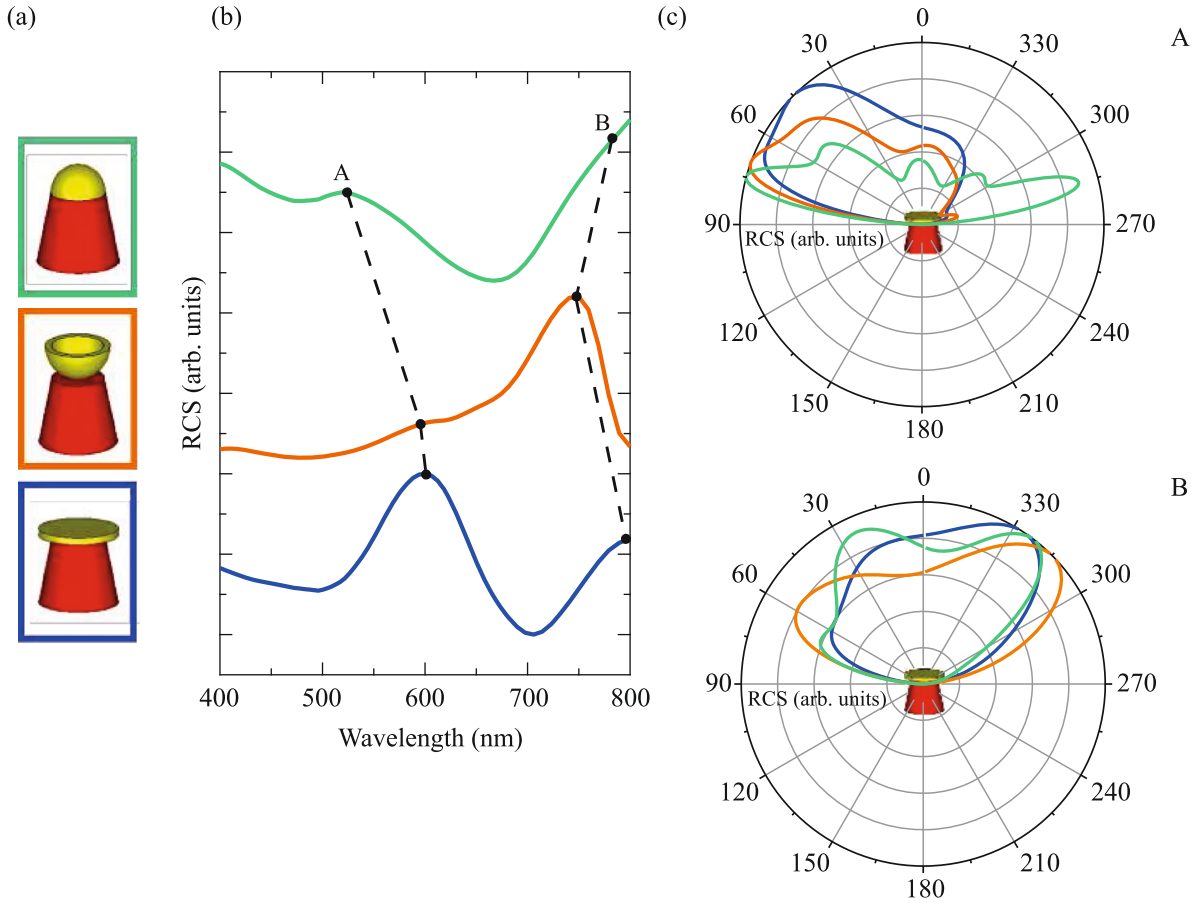

Fig. 3. (Color online) (a) Schematic view of hybrid structures with the gold component of disk, cup, and hemisphere shapes (i.e., before and after reshaping), (b) its calculated scattering cross-sections, and (c) light scattering diagrams at A and B spectral positions corresponding to local maximum points; spectrum color in (b) denotes the state of the hybrid structure shown in (a).

ence up to 80 mJ/cm^2 it transforms to a semi-spherical shape. In addition, it can be seen that the unmodified nanostructures are still retaining their original shape. At the same time, precise modification of gold component geometric parameters is possible by femtosecond laser-induced reshaping.

Figure 2b presents measured scattering spectra of hybrid nanostructures with different degrees of modification. As demonstrated in Fig. 2, unmodified nanostructures and modified at below 20 mJ/cm^2 share the same resonance, while scattering spectra start to change their profile for structures exposed with fluences higher than 40 mJ/cm^2. In particular, this modification results in the blue shift of optical resonance, which is highly consistent with simulations.

To support obtained experimental results, numerical simulations of optical properties were done. Properties of the hybrid nanostructures in the optical frequency range and scattering patterns have been studied numerically using CST Microwave Studio. Simulation parameters are consistent with experimental dimensions. The electromagnetic plane wave is obliquely illuminated on the studied hybrid nanostructure on glass substrate at the angle of 68 degrees along the z-axis, i.e., symmetry axis of the structures. The collecting signal is limited to a short-range from the top in consistency with the experimental collection objective.

Here, we consider the scattering properties of a single hybrid nanoparticle consisting of Si nanocone and Au nanodisk. The bottom and top base diameters of Si nanocone are equal to 240 and 160 nm, respectively. We assume that the diameter of Au nanodisk is equal to the diameter of the lower base of the Si nanocone, which is dictated by the lithography process (i.e., 240 nm, Fig. 3a). The height of a nanocone is equal to 200 nm. We also take that the thickness of the Au nanodisk is equal to 20 nm. Considering that the volume of gold is constant, for the cup shape of the gold component, we take the hollow sphere with a wall thickness of 20 nm and an outer radius of 94.7 nm. The geometric parameter of the hemisphere shape is the radius, which is equal to 75.6 nm. Materials properties are taken from [18] for the gold dispersion model and [19] for the amorphous silicon. Figure 3 shows the simulated scattering cross-section and radiation pat-

tern of hybrid nanostructures with different amounts of modifications.

As demonstrated in Fig. 3, with the shape of the gold component varying from disk to cup, the localized surface plasmon resonance (LSPR) generated from gold nanostructures as well as the mode interactions between the metal and dielectric counterparts are modified. The LSPR peak exhibits a moderate blue shift while the interaction mode is reconfigured. This phenomenon is also observed within the process of cup reshaping to the hemisphere. LSPR is strongly dependent on the shape of metallic nanoparticles; thus, LSPR can be precisely tuned in the visible range by controlling the femtosecond-laser intensity, which irradiates on the hybrid nanostructure and results in different shapes of the metal component. In addition, LSPR typically demonstrates a broadband resonance lacking the ability to control the radiation, as shown in Fig. 3c. The scattering diagrams of three hybrid configurations at resonance B presents similar radiation in the far-field. In opposite, resonance A identifies the interactions of plasmonic and electric modes and demonstrates narrower band radiation with the process of femtosecond-laser reshaping, as depicted in Fig. 3c.

Both experimental results and the theoretical calculations indicate a strong blue shift of the broadband magnetic resonance ($\Delta_A > 70$ nm), indicated as A and a minor blue shift of the plasmon resonance ($\Delta_B \approx 20$ nm), indicated as B in Figs. 2 and 3.

In conclusion, the evolution of scattering properties enabled by femtosecond-laser reshaping shows the potential of hybrid metal–dielectric nanostructures for color printing applications. The reshaping process can tune the resonance of the nanostructure in the whole visible wavelength range resulting in different colors of illuminated nanostructures ranging from yellow through green to red. Therefore it is possible to change the color after the fabrication of initial nanostructures by lithographic techniques. Such tuning can be enhanced by the presence of resonances from both gold and silicon parts. Moreover, color tuning is simultaneously accompanied by alteration in light scattering patterns. This kind of tunable hybrid nanostructures is promising not only for color printing applications but also in sensors or biomedical applications.

FUNDING

This work was supported by the Russian Science Foundation (project no. 19-79-10259).

CONFLICT OF INTEREST

The authors declare that they have no conflicts of interest.

OPEN ACCESS

REFERENCES

1. S. Daqiqeh Rezaei, Z. Dong, J. You En Chan, J. Trisno, R. J. H. Ng, Q. Ruan, C.-W. Qiu, N. A. Mortensen, and J. K. W. Yang, ACS Photon. **8**, 18 (2020).
2. M. Song, D. Wang, S. Peana, S. Choudhury, P. Nyga, Z. A. Kudyshev, H. Yu, A. Boltasseva, V. M. Shalaev, and A. V. Kildishev, Appl. Phys. Rev. **6**, 041308 (2019).
3. A. Kristensen, J. K. W. Yang, S. I. Bozhevolnyi, S. Link, P. Nordlander, N. J. Halas, and N. A. Mortensen, Nat. Rev. Mater. **2**, 1 (2016).
4. T. Lee, J. Jang, H. Jeong, and J. Rho, Nano Convergence **5**, 1 (2018).
5. B. Yang, H. Cheng, S. Chen, and J. Tian, Mater. Chem. Front. **3**, 750 (2019).
6. K. L. Kelly, E. Coronado, L. L. Zhao, and G. C. Schatz, J. Phys. Chem. B **107**, 668 (2002).
7. C. U. Hail, G. Schnoering, M. Damak, D. Poulikakos, and H. Eghlidi, ACS Nano **14**, 1783 (2020).
8. T. Chen and B. M. Reinhard, Adv. Mater. **28**, 3522 (2016).
9. S. D. Rezaei, R. J. Hong Ng, Z. Dong, J. Ho, E. H. H. Koay, S. Ramakrishna, and J. K. W. Yang, ACS Nano **13**, 3580 (2019).
10. J.-H. Yang, V. E. Babicheva, M.-W. Yu, T.-C. Lu, T.-R. Lin, and K.-P. Chen, ACS Nano **14**, 5678 (2020).
11. V. Flauraud, M. Reyes, R. Paniagua-Domínguez, A. I. Kuznetsov, and J. Brugger, ACS Photon. **4**, 1913 (2017).
12. Y. Nagasaki, M. Suzuki, I. Hotta, and J. Takahara, ACS Photon. **5**, 1460 (2018).
13. S. Sun, Z. Zhou, C. Zhang, Y. Gao, Z. Duan, S. Xiao, and Q. Song, ACS Nano **11**, 4445 (2017).
14. N. Maccaferri, A. Zilli, T. Isoniemi, L. Ghirardini, M. Iarossi, M. Finazzi, M. Celebrano, and F. de Angelis, ACS Photon. **8**, 512 (2021).
15. D. A. Zuev, S. V. Makarov, I. S. Mukhin, V. A. Milichko, S. V. Starikov, I. A. Morozov, I. I. Shishkin, A. E. Krasnok, and P. A. Belov, Adv. Mater. **28**, 3087 (2016).
16. Y. Sun, S. Kolodny, S. Lepeshov, D. Zuev, L. Huang, P. Belov, and A. Krasnok, Ann. Phys. **529**, 1600272 (2016).
17. S. Lepeshov, A. Krasnok, I. Mukhin, D. Zuev, A. Gudovskikh, V. Milichko, P. Belov, and A. Miroshnichenko, ACS Photon. **4**, 536 (2017).
18. P. B. Johnson and R. W. Christy, Phys. Rev. B **6**, 4370 (1972).
19. D. T. Pierce and W. E. Spicer, Phys. Rev. B **5**, 3017 (1972).